ORIGINAL PAPER

Formation of cuprous oxide layers in Cu(II) solutions containing gluconic acid

Arvydas Survila · Jolanta Pileckienė ·
Stasė Kanapeckaitė · Putinas Kalinauskas ·
Giedrius Stalnionis

Abstract In accordance with thermodynamic analysis, cuprous oxide layers are formed spontaneously in the Cu|Cu (II), gluconic acid system at pH>3.7 under open-circuit conditions. A current peak of Cu_2O reduction is observed on cathodic voltammograms at ca −0.7 V, its height being dependent on the exposure time. The analysis of the charge transferred in this region yields the rate of Cu_2O formation equal to 1.25×10^{-10} mol cm^{-2} s^{-1}. The light perturbation of Cu electrode under open-circuit conditions results in the generation of a negative photopotential, which is indicative of n-type conductivity. The threshold wavelength is equal to ~590 nm and is consistent with a band gap of ~2.1 eV. Anodic photocurrents, which are observed near the open-circuit potential, decrease with cathodic polarization and change their sign at ~0.05 V. Analysis of impedance data was performed, invoking the equivalent circuit that accounts for the two-step charge transfer. In the presence of Cu_2O, some retardation of Cu(II) reduction was found to occur with a slight increase in the admittance of the double layer. The suggestion has been made that oxide layers formed in Cu(II) gluconate solutions cannot be compact and uniformly distributed over the entire electrode surface. Relevant investigations of surface morphology support this conclusion.

Keywords Cuprous oxide · Gluconic acid · Photoresponse · Impedance

A. Survila (✉) · J. Pileckienė · S. Kanapeckaitė · P. Kalinauskas ·
G. Stalnionis
Center for Physical Sciences and Technology,
Institute of Chemistry,
A. Goštauto 9,
01108 Vilnius, Lithuania
e-mail: arvydass@ktl.mii.lt

Introduction

Cuprous oxide layers developed in electrochemical systems often show the features that are not typical of monocrystals or polycrystalline compacts. First of all, the so-called anomalous n-type conductivity of Cu_2O surface layers is often observed [1–7]. Various reasons for such an effect have been discussed including certain peculiarities of thin layers [8] or deviations from the stoichiometry in oxygen containing layers [1, 4, 9]. It has also been established that the aforementioned deviations vary with the depth of oxide layer. For this reason, the types of conductivity observed at the Cu|Cu_2O and Cu_2O|solution boundaries can be different [4, 10].

Much attention has recently been focused on the layers formed in electrochemical systems containing ligands that are capable of forming various Cu(II) complexes. Spontaneous processes occurring in such systems under open-circuit conditions, as well as the conditions for Cu_2O formation, have been analyzed [11]. It has been established that the nature of ligands as well as the composition of ligand-containing solutions can have a pronounced effect on kinetics of oxide formation and the properties of the layers obtained [6]. Both n- and p-type oxides can be formed in the presence of ligands.

Prospects for practical implementation of semiconducting Cu_2O layers have also been the object of considerable attention. Hara et al. considered [12] that the illuminated particles or specially fabricated films of cuprous oxide can serve as an effective catalyst for decomposition of water. DeJongh et al. suggested [13] to use Cu_2O as a cathode in photovoltaic cells. However, it has been questioned [14] whether cuprous oxide could be successfully used for utilization of light energy, since this substance is liable to photocorrosion being unstable both

cathodically and anodically [5, 7, 15, 16]. Still and all, an idea to use cuprous oxide in solar cells remains popular [17–21].

At present, there is no doubt that (photo)electrochemical properties of Cu_2O strongly depend on the conditions under which they are built up. This paper deals with further investigations of the main regularities concerning cuprous oxide layers spontaneously developed in ligand-containing systems. For this purpose, the Cu|Cu(II), gluconic acid system containing an ecological ligand has been chosen.

Experimental

Solutions under investigation contained 0.01 M $CuSO_4$ (Mallinckrodt, USA), 0.02 or 0.04 M sodium gluconate $NaC_6H_{11}O_7$ (Sigma-Aldrich, 99% purity), and 0.3 M K_2SO_4 (Reakhim, Russia, high purity) as a supporting electrolyte. Specified values of pH, equal to 3.0 or 5.0, were adjusted by addition of H_2SO_4 or KOH. Twice-distilled water was used to prepare solutions. A pure argon stream was passed through solutions for 0.5 h prior to measurements. All experiments with the solutions were carried out at 20 °C.

To prepare working electrodes, a platinum disc (voltammetric measurements) or wire (impedance measurements) was coated with a 5- to 7-µm-thick copper layer in the solution containing: $CuSO_4 \cdot 5\ H_2O$—200 g dm^{-3} and H_2SO_4—50 g dm^{-3} at 10 mA cm^{-2}. The working electrode was rinsed with water, immediately immersed into the solution under investigation and kept in it for the controlled time τ. Electrode potentials were measured with respect to the Ag|AgCl|KCl(sat) reference electrode and were converted to the standard hydrogen scale.

Voltammograms were recorded at the potential sweep rate $v=5$ mV s^{-1} using a potentiostat PI-50-1 (Belorussia).

A special cell was used for photoelectrochemical experiments. Uniformly focused monochromatic light was directed at the working electrode through a quartz window. Operating wavelengths of 3 W light-emitting diodes (Future Electronics) were as follows: 455, 470, 505, 530, 590, 617, and 627 nm. The power density of illumination (300 mW cm^{-2}) was controlled with an LM-2 device (Carl Zeiss Jena, Germany). The response of electrochemical system to optical perturbation was investigated in two ways. In the first case, the dynamics of the photopotential under open-circuit conditions were recorded. The second case involved recording voltammograms while perturbing with regularly repeating light pulses.

An electrochemical cell equipped for EIS measurements contained an extra platinum cylinder (~6 cm^2) that was used as an auxiliary electrode for polarization with alternating current. Measurements were carried out under potentiostatic conditions (the open-circuit potential was maintained) within the frequency (f) range from 0.05 to 5×10^4 Hz using a Zahner Elektrik (Germany) IM6 Impedance Spectrum Analyzer. Computer programs elaborated by Boukamp [22] were used for analyzing impedance spectra.

The analysis of the surface of specimens was accomplished by using a scanning electron microscope ZEISS EVO-50 at an accelerating voltage of 20 kV. Average analysis data were obtained from the surface site 0.5×0.5 mm in size.

Results and discussion

Cuprous oxide layers may be easily formed on the surface of copper electrode when it is exposed to the solution containing Cu(II) complexes. At first, the reversible process

$$Cu + Cu^{2+} \rightleftarrows 2Cu^+ \qquad (1)$$

proceeds resulting in the saturation with Cu^+ ions of the solution layer adjacent to the electrode surface. If their concentration exceeds a certain maximum value determined by the condition [23]

$$\log[Cu^+]_{max} = -0.84 - pH, \qquad (2)$$

an unstable CuOH is formed with its following decomposition into Cu_2O and H_2O. The net process may be written as

$$Cu + Cu^{2+} + 2OH^- \rightarrow Cu_2O + H_2O. \qquad (3)$$
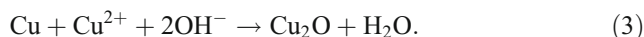
Quite deep chemical conversions may occur in the system as long as the total equilibrium state is attained. Then, condition (2) can be modified using the equilibrium constant K of process (1). According to the Nernst equation

$$K = \frac{[Cu^+]^2}{[Cu^{2+}]} = \exp\left[\frac{2F}{RT}(E_{20} - E_{10})\right], \qquad (4)$$

where the standard potentials of the $Cu^+|Cu$ and $Cu^{2+}|Cu$ electrodes, E_{10} and E_{20}, are equal to 0.521 and 0.337 V, respectively [24]; then $K=4.5 \times 10^{-7}$. With this value, it follows from (2) to (4) that

$$\log[Cu^{2+}]_{max} = 4.67 - 2pH. \qquad (5)$$

To check the latter condition, the determination of the solution composition should be made. Spectrophotometric investigations of acidic $CuSO_4$ solutions containing gluconic acid have shown [25] that the following species are sufficient to be considered at pH<6:

1. Cu(II) complexes, viz., "free" Cu^{2+} ions (aqua complexes), the monoligand gluconate complex CuL^- and ionic pair (sulfate complex) $CuSO_4$;

2. Active forms of ligands capable of forming coordination bonds with Cu^{2+} ions, viz., gluconate L^- and sulfate SO_4^{2-};

3. Protonated ligands, viz., LH (gluconic acid) and HSO_4^-.

To obtain the distribution of different species in the system under discussion, material balance equations, accounting for total Cu(II), gluconate, and sulfate, were set up. Besides, appropriate stability constants were used; their values may be found in Ref. [25]. An example of the results obtained is presented in Fig. 1. The dashed line separates two areas. When pH$\lesssim$4, the probability of Cu_2O formation is low; the cuprous oxide becomes thermodynamically stable in the right part of the diagram. Due to a moderate degree of Cu(II) complexation, the ligand concentration slightly affects the pH of Cu_2O formation. Special experiments have shown that the surface Cu_2O can be formed when solution pH exceeds ~3.7.

Surface oxide layers can be detected in a number of ways. One of them lies in the fact that Cu_2O is capable of reduction. When the electrode process

$$Cu_2O + 2H^+ + 2e \rightarrow 2Cu + H_2O, \tag{6}$$

occurs, a characteristic current peak arises at $E \approx -0.7$ V in some systems containing Cu(II) complexes [7, 11, 26]. Its height varies linearly with the potential sweep rate v [11] and depends on the exposure time τ. These phenomena are also typical of the system under discussion.

Cathodic voltammograms obtained at different τ are given in Fig. 2; an example of cyclic voltammogram is shown in the inset. When the Cu electrode is exposed to the Cu(II) solution for less than 5 min, no current peak is
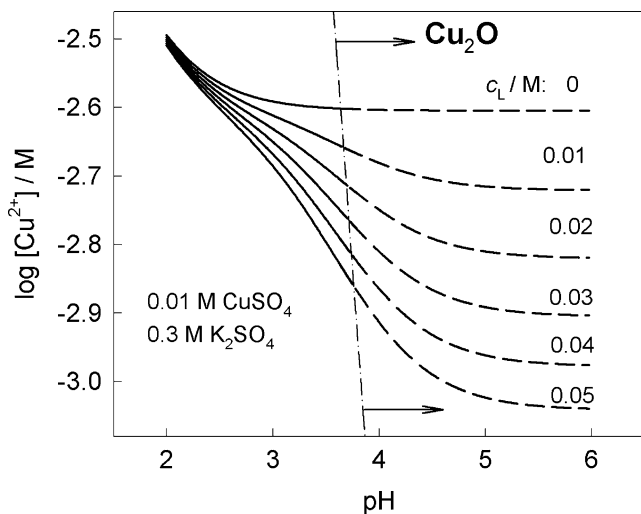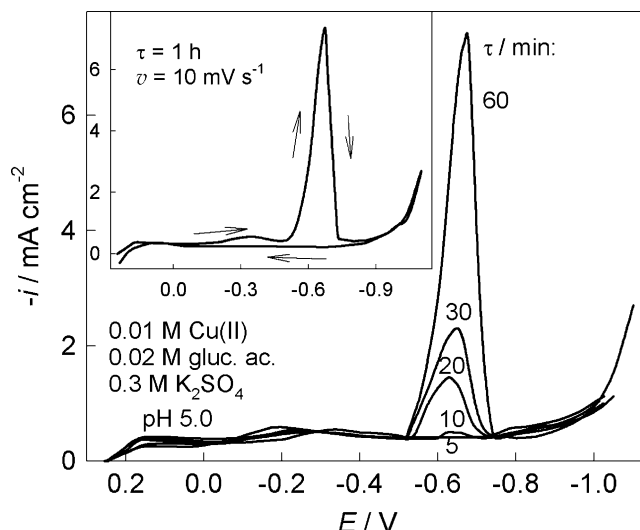

Fig. 2 Cathodic voltammograms obtained for the solutions of indicated composition at different exposure times τ that are given at the respective *curves*. An example of cyclic voltammogram is shown in the *inset*

observed. However, at longer exposure times, the critical Cu^+ concentration is accumulated and the formation of Cu_2O becomes possible. Considering the absence of current peaks on the reverse voltammograms (see inset in Fig. 2), it can be concluded that Cu_2O is fully reduced during the direct potential scan. Then, the charge Q obtained from the integration of current peak could serve as a measure of the amount of surface oxide. It can be seen from Fig. 3 that the incubation takes 6 to 7 min until the onset of increasing Q is observed. The rate dQ/dt develops with time approaching the value equal to 24 μC cm^{-2} s^{-1}. Taking into account the stoichiometry of the process (6), the rate of Cu_2O formation can be expressed as follows:

$$v_{Cu_2O} = \frac{1}{2F} \frac{dQ}{dt}. \tag{7}$$

Then, the steady $v_{Cu_2O} = 1.25 \times 10^{-10}$ mol cm^{-2} s^{-1}. It is interesting to note that a similar rate was also obtained in the case of Cu(II)–ethylenediamine system [11]. On average, less than two monolayers could be formed over 1 min.

Another way for Cu_2O detection is based on its sensitivity to light perturbation. The cuprous oxide belongs to *p*-type semiconductors with a band gap of ~2.1 eV [2] that is consistent with the threshold wavelength (λ_{max}) equal to ~590 nm. The light perturbation of Cu electrode under open-circuit conditions results in the generation of a negative photopotential (Fig. 4), which is indicative of *n*-type conductivity. This type is not characteristic of Cu_2O monocrystals or polycrystalline compacts but it is rather common in the electrochemical systems. Photopotential

Fig. 1 Dependences of Cu^{2+} concentration on pH calculated for the solutions containing 0.01 M of $CuSO_4$, 0.3 M of K_2SO_4, and different concentrations of gluconic acid (c_L) that are indicated at the respective curves. *Dashed lines* fall into the region where Cu_2O is thermodynamically stable
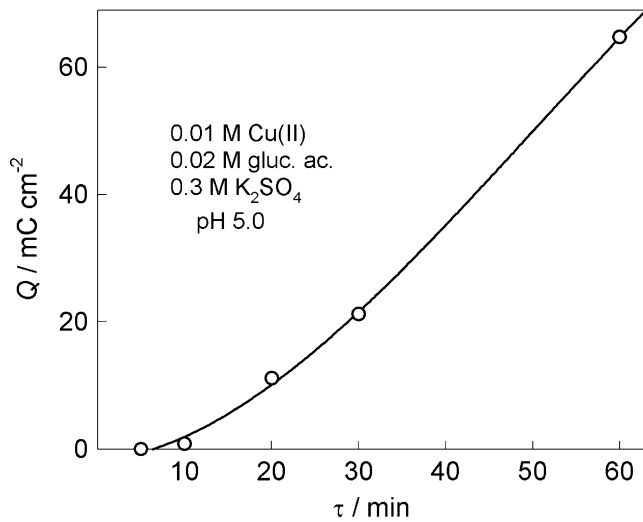
Fig. 3 The charge used for reduction of oxide layers formed at different exposure times τ. Results of integration of the cathodic current peaks given in Fig. 2

Fig. 5 Examples of cathodic voltammograms obtained under chopped illumination conditions at exposure times equal to 30 min (ordinate to the right) and 60 min (ordinate to the left). λ=455 nm, N= 300 mW cm^{-2}

pulses obviously depend on the quantum energy and decrease with the wavelength. The photoresponse disappears at ~590 nm that is consistent with the λ_{max} given above. Moreover, the result obtained is indicative of the band gap similar to that established for stoichiometric p-type Cu$_2$O crystals.

The response of the oxide layers to optical perturbation manifests itself under cathodic polarization conditions as well (Fig. 5). In accordance with n-type conductivity, anodic photocurrents are observed at $E>0.05$ V. The highest response is generated near the open-circuit potential. When oxide layers are formed sufficiently long (60 min), the anodic pulses can range up to 20 mA cm^{-2}. It is conceivable that this is the most intense response of

Cu$_2$O layers formed in electrochemical systems to the present day.

As the cathodic polarization is increased, the photocurrent weakens, disappears, whereupon the opposite in sign current emerges again (Figs. 5 and 6). The inversion potential (E_{inv}) is located at ~0.05 V. Its more accurate position depends to some extent on the exposure time and, consequently, on the thickness of oxide layer. Such phenomena are typical of the most Cu(II) systems with some quantitative distinctions. For example, in the case of Cu(II)–gluconic acid solutions, E_{inv} is more negative and approaches −0.2 V [27].
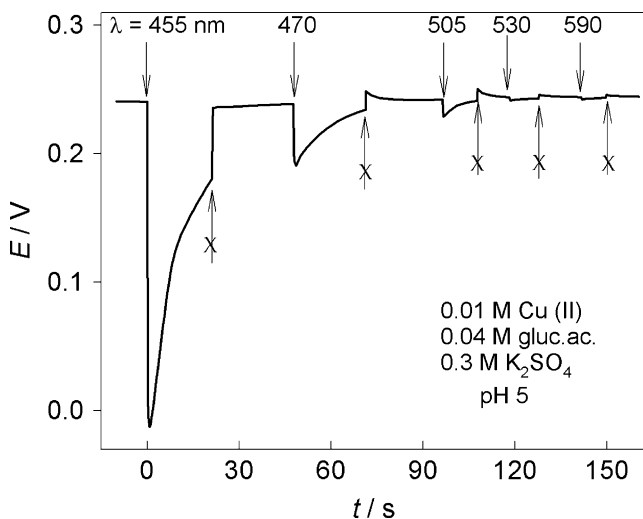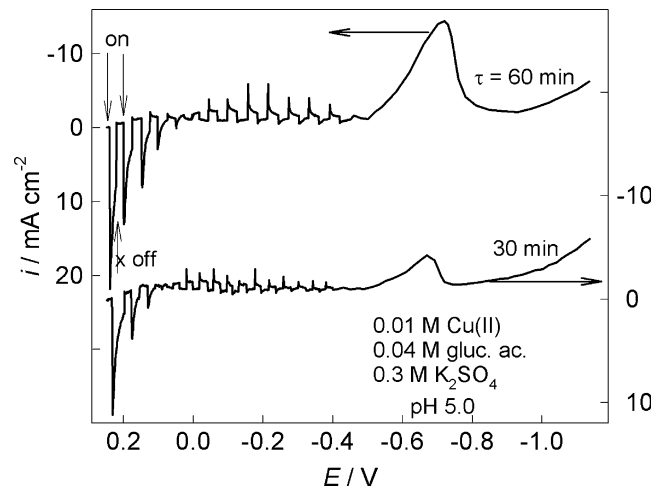

Fig. 4 Photopotential generated with light pulses of different wavelengths. Respective *arrows* indicate the start and the end of light perturbation. The Initial exposure time τ=10 min
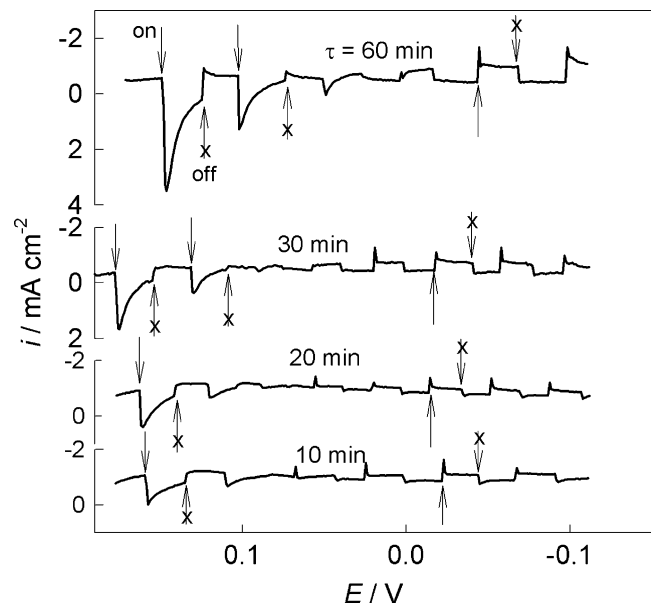

Fig. 6 Regions of inversion of photocurrent sign. The voltammetric data were obtained at different exposure times, which are indicated at the respective voltammograms

Formation of oxide layers has a certain effect on the impedance characteristics. This can be seen from the data shown in Fig. 7. Three records of the impedance correspond to the exposure times τ equal to 5, 15, and 25 min, respectively. For the most part, Nyquist plots (the interrelations between real, Z', and imaginary, Z'', impedance components) present the arcs (a quarter of circle) centered below the abscissa axis. Contrary to ethylenediamine or β-alanine systems [7], no extra arcs or inductive loops arise from oxidation of electrode surface. At both pHs, the duration of stay of Cu electrode in the solution somewhat affects the experimental data: the impedance increases with the exposure time τ. It should be mentioned that a full record of impedance spectra lasts about 8 min, but the record of its major part (at $f > 10$ Hz) takes only some tens of seconds. The application of Kramers–Kronig transforms at pH 3.0 has shown [28] that transformed and experimental data coincide quite well over a large area of frequencies applied, viz., at $f > 3$ Hz. Hence, the results, obtained in this region, relate to a sufficiently stable system, even though the steady state is not reached.

To obtain kinetic and double-layer characteristics, an appropriate equivalent circuit (EC) of the interphase electrode|solution was selected. It is well known that the electrochemical reduction of Cu(II) involves two consecutive charge transfer steps resulting in the formation of intermediate Cu(I) compounds. In this case, the faradaic part of EC is represented by two parallel sub-circuits, each containing the charge transfer resistance (R) and Warburg impedance (W) in series [29]. Next, the faradaic impedance

Fig. 7 Nyquist plots obtained at open-circuit potential for the solutions containing 0.01 M of Cu(II) and 0.04 M of gluconic acid at pH 3.0 (*upper part*) and 5.0 (*lower part*). The experimental data (*symbols*) are compared with those simulated for the indicated equivalent circuit (*lines*)

is shunted with the capacitance of the double electric layer (C_{dl}), and finally, the ohmic resistance of the solution (R_Ω) is attached. Following the Boukamp's symbolism [22], the description code of this circuit is: R_Ω ($C_{dl}[R_1W_1][R_2W_2]$) (here, elements in series are written in angle brackets and parallel elements are given in parenthesis).

We slightly modified such EC, replacing C_{dl} by the constant phase element (CPE) Q_{dl}. According to the definition [30, 31], the admittance (Y_{dl}) of Q_{dl} can be expressed as follows:

$$Y_{dl} = Y_0(j\omega)^n, \qquad (8)$$

where $\omega = 2\pi f$, $j = \sqrt{-1}$. When the index n is equal to 1, 0.5, or 0, the CPE transforms into the capacitance, Warburg impedance, or resistance, respectively.

Fitting procedures were applied to obtain parameters of EC elements; they are summarized in Table 1. At pH 3.0, this circuit enabled us to describe experimental data quantitatively with a frequency error of 2–3% over the range from 0.3 Hz to 30 kHz. The results, obtained at pH 5.0, are somewhat worse (Fig. 7). Nevertheless, a certain semi-quantitative comparison of the data, obtained at different pH, seems to be possible.

In the case of oxide-free copper surface, the following relationships, obtained in [29], may be used for estimation of exchange current densities i_{01} and i_{02}:

$$i_{01} + i_{02} = \frac{RT}{F}\left(\frac{1}{R_1} + \frac{1}{R_2}\right), \qquad (9)$$

$$\frac{1}{i_{01}} + \frac{1}{i_{02}} = \frac{R_1 + R_2}{\sigma_1 + \sigma_2}\frac{1}{F\sqrt{D}}\left(\frac{1}{[Cu^{2+}]} + \frac{4}{[Cu^+]}\right), \qquad (10)$$

where σ_1 and σ_2 are coefficients of the respective Warburg impedances (see EC elements W_1 and W_2). They are defined according to the general equation [30, 31]

$$Z_W = \sigma(1-j)/\sqrt{\omega}, \qquad (11)$$

Then, Warburg admittance

$$Y_W \equiv (Z_W)^{-1} = Y_0\sqrt{j\omega} = Y_0(1+j)\sqrt{2\omega}/2 \qquad (12)$$

and

$$\sigma = \left(\sqrt{2}Y_0\right)^{-1}. \qquad (13)$$

Hence, σ_1 and σ_2 can be easily obtained from Y_{01} to Y_{02} quantities given in Table 1. Equilibrium concentration of Cu^{2+} ions ($[Cu^{2+}] = 2.14$ mM) was obtained using well-known material balance equations and stability constants determined and listed in Ref. [25]. It follows from the analysis of standard potentials of Cu|Cu^{2+} to Cu|Cu^+ electrodes that the equilibrium constant of the process $Cu + Cu^{2+} \leftrightarrows 2\ Cu^+$ is equal to
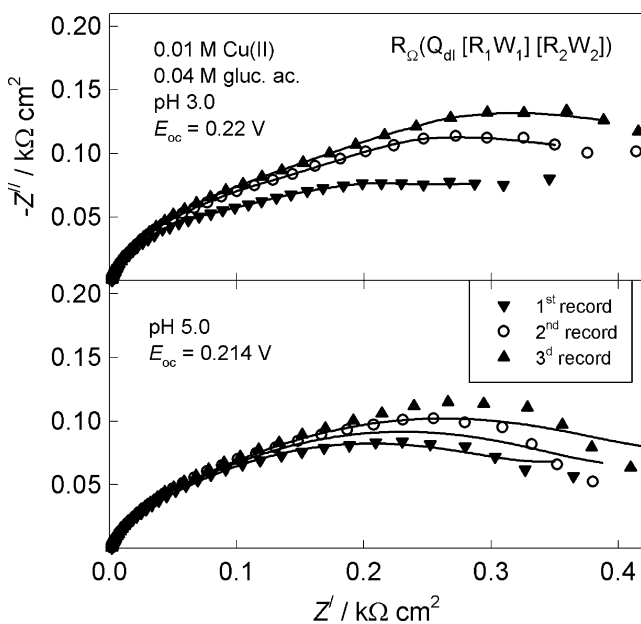
Table 1 Parameters of the equivalent circuit R_Ω (Q_{dl} [$R_1 W_1$] [$R_2 W_2$]) determined at $0.3 < f < 30{,}000$ Hz

E/V	τ/min	Q_{dl}		R_1	W_1	R_2	W_2	Note
		$10^5\ Y_0$	n	R_1	$10^3\ Y_{01}$	R_2	$10^4\ Y_{02}$	
pH 3.0								
0.221	5	9.59	0.815	273	9.72	84.4	7.49	1st record
	15	7.41	0.833	343	6.15	70.2	6.06	2nd record
	25	6.79	0.839	375	4.92	65.7	5.69	3rd record
Relative error, %		7	1	6	12	6	7	
pH 5.0								
0.214	5	12.6	0.795	375	42.8	69.1	9.03	1st record
	15	11.0	0.802	429	59.0	81.7	8.53	2nd record
	25	11.2	0.800	481	53.9	88.2	8.83	3rd record
Relative error, %		8	1	4	60	11	5	

Dimensions: $[R] = \Omega\ \mathrm{cm}^2$, $[Y_0] = \Omega^1\ \mathrm{cm}^{-2}\ \mathrm{s}^n$, $[Y_{01}] = [Y_{02}] = \Omega^1\ \mathrm{cm}^{-2}\ \mathrm{s}^{0.5}$

4.5×10^{-7} M; then $[\mathrm{Cu}^+] = 3.1 \times 10^{-5}$ M. The value of the diffusion coefficient $D = 4 \times 10^{-6}\ \mathrm{cm}^2\ \mathrm{s}^{-1}$ was also taken from Ref. [25]. Simulations, carried out by Eqs. (9) and (10), yield the following values of i_{01} and i_{02}: 4.30 and 383 $\mu\mathrm{A}\ \mathrm{cm}^{-2}$ (first record), 4.69 and 424 $\mu\mathrm{A}\ \mathrm{cm}^{-2}$ (second record), and 4.75 and 442 $\mu\mathrm{A}\ \mathrm{cm}^{-2}$ (third record). It can be seen primarily that $i_{01} \ll i_{02}$, i.e., the transfer of the first electron is the rate-determining step. Secondly, the variations in i_0 are rather low as compared with the changes in Y_0 (see element Q_{dl} in Table 1). Thus, it could be concluded that the certain restructuring of the double layer has a rather weak effect on the exchange current densities. The settled $i_{01} = 4.8\ \mu\mathrm{A}\ \mathrm{cm}^{-2}$ is consonant with similar quantities obtained from voltammetric data [25].

It should be noted that n values relating to the admittance of double layer are less than 1 (Table 1). The roughness of copper coatings should be mentioned as one of the factors responsible for such a feature. Besides, it is conceivable that Q_{dl} stands for a more complex sub-circuit that characterizes a non-equilibrium double layer. The attempts to elucidate its structure have failed, since the addition of extra elements overloads the basic EC and renders its analysis impossible. Despite all complications, we can safely assume that the admittance of the double layer formed in the presence of oxides is higher as compared with that of bare copper. This means that oxide layers formed in Cu(II) gluconate solutions cannot be compact and uniformly distributed over the entire electrode surface; otherwise, low capacitances typical of semiconductors should be detected. Clearly the adsorption properties of bare and oxidized electrodes differ to a certain extent. The diminution of Y_0 with τ intimates that the adsorption of gluconate intensifies and the double-layer capacitance decreases.

Since the foregoing equations were derived for equilibrium conditions and do not account for the formation of oxide layers,

their use at pH 5.0 becomes problematic. Nevertheless, it can be stated that the charge transfer resistances are higher in the latter case (Eqs. (9) and (10) yield twice lower i_{01} values). This
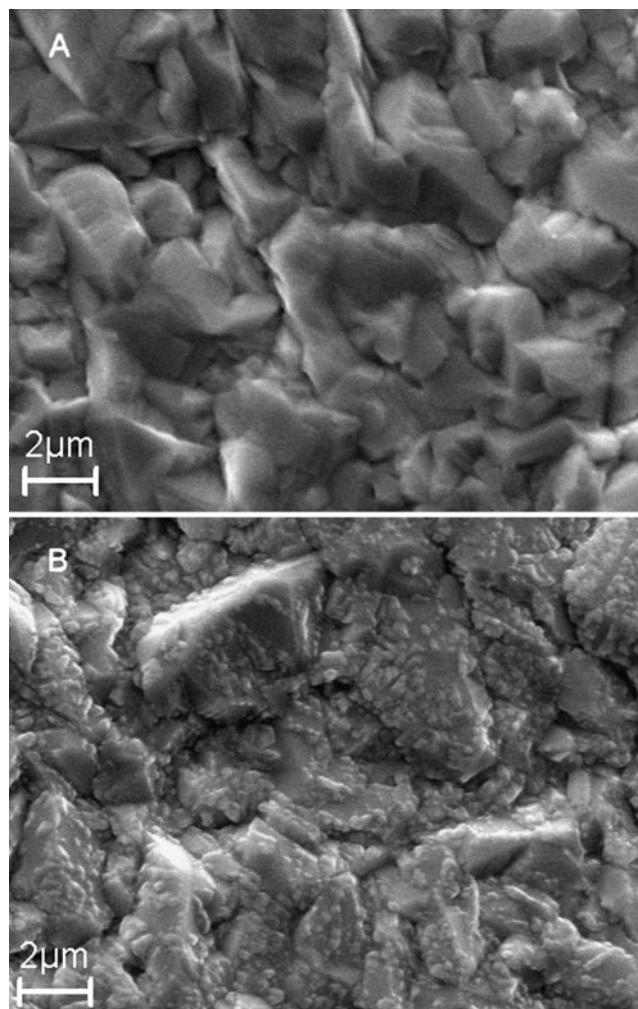
Fig. 8 Morphology of freshly prepared copper coating (**a**) and of that exposed for 30 min in the gluconate-containing Cu(II) solution (**b**)

means that the formation of Cu$_2$O results in some retardation of Cu(II) reduction.

SEM micrographs of freshly prepared copper coating (part a) and of that exposed for 30 min to the gluconate-containing Cu(II) solution (part b) are shown in Fig. 8. A polycrystalline layer with well-exhibited crystallographic edges and faces is formed during preparation of the working electrode. Copper crystallites as large as 1–4 μm cover a great part of the surface and impart a particular roughness that manifests itself in the impedance measurements. No oxygen was detected on such coatings. As the exposure time τ increases, the amount of surface oxygen increases as well. As this takes place, the tendency of segregation of Cu$_2$O is observed. A typical result of such a process can be seen from Fig. 8b. Cu$_2$O crystallites, ~50–140 nm in size, are distributed nonuniformly and seem to cover some steps and kink and other sites that are most liable to anodic dissolution. Bare copper is visible between Cu$_2$O crystallites. Thus, it is evident that the electrochemical properties of electrode surface cannot change drastically when the compact semi-conducting layer is not formed.

Conclusions

In accordance with the thermodynamic analysis, cuprous oxide layers are formed spontaneously in the Cu|Cu(II), gluconic acid system at pH>3.7 under open-circuit conditions. A current peak of Cu$_2$O reduction is observed on cathodic voltammograms at ca −0.7 V, its height being dependent on the exposure time. An analysis of the charge transferred in this region yields the rate of Cu$_2$O formation equal to 1.25×10^{-10} mol cm^{-2} s^{-1}. The light perturbation of Cu electrode under open-circuit conditions results in the generation of a negative photopotential, which is indicative of n-type conductivity. The threshold wavelength is equal to ~590 nm and is consistent with a band gap of ~2.1 eV. Anodic photocurrents, which are observed near the open-circuit potential, decrease with cathodic polarization and change their sign at ~0.05 V.

Analysis of impedance data was performed, invoking the equivalent circuit that accounts for the two-step charge transfer. In the presence of Cu$_2$O, some retardation of Cu(II) reduction was found to occur with a slight increase in the admittance of the double layer. The suggestion has been made that oxide layers formed in Cu(II) gluconate solutions cannot be compact and uniformly distributed over the entire electrode surface. Relevant investigations of surface morphology support this conclusion.

References

1. Pointu B, Braizaz H, Poncet P, Rousseau J (1983) J Electroanal Chem 151:65
2. Aruchamy A, Fujishima A (1989) J Electroanal Chem 266 (397):272–125
3. Survila A, Kalinauskas P, Uksienė V (1993) Electrochim Acta 38:2733
4. Millet B, Fiaud C, Hinnen C, Sutter EMM (1995) Corros Sci 37:1903
5. Survila A, Kalinauskas P, Ivaškevič E, Kutner W (1997) Electrochim Acta 42:2935
6. Survila A, Kalinauskas P, Valsiūnas I (2002) Russ J Electrochem 38:1068
7. Survila A, Survilienė A, Kanapeckaitė S, Būdienė J, Kalinauskas P, Stalnionis G, Sudavičius A (2005) J Electroanal Chem 582:221
8. Bertocci U (1978) J Electrochem Soc 125:1598
9. Babić R, Metikoš-Huković M, Lončar M (1999) Electrochim Acta 44:2413
10. Survila A, Kalinauskas P, Survilienė A, Sudavičius A (2007) Chemija (Vilnius) 18:18
11. Survila A, Kanapeckaitė S, Survilienė A (2001) J Electroanal Chem 501:151
12. Hara M, Kondo T, Komoda M, Ikeda S, Shinohara K, Tanaka A, Kondo J, Domen K (1998) J Chem Soc, Chem Commun 3:357
13. DeJongh PE, Vanmaekelbergh D, Kelly JJ (2000) J Electrochem Soc 147:486
14. Rajeshwar K, Singh P, DuBow J (1978) Elchim Acta 23:1117
15. Gerischer H (1977) J Electroanal Chem 82:133
16. Survila A, Kalinauskas P, Uksienė V (1988) Chemija (Vilnius) 1:51
17. Ishizuka S, Kato S, Okamoto Y, Sakurai T, Akimoto K, Fujiwara N, Kobayashi H (2003) Appl Surf Sci 216:94
18. Mahalingam T, Chitra JSP, Chu JP, Sebastian PJ (2004) Mater Lett 58:1802
19. Rai BP (1988) Sol Cells 25:265
20. Nakaoka K, Ueyama J, Ogura K (2004) J Electrochem Soc 151:C661
21. Mahalingam T, Chitra JSP, Chu JP, Moon H, Kwon HJ, Kim YD (2006) J Mater Sci Mater Electron 17:519
22. Boukamp BB (1989) Equivalent circuit (EQUIVCRT.PAS). User's manual. University of Twente, Enschede
23. Pourbaix M (1966) Atlas of electrochemical equilibria in aqueous solution. Pergamon, London
24. Bard AJ, Parsons R, Jordan J (eds) (1985) Standard potentials in aqueous solution. Marcel Dekker, New York
25. Survila A, Mockus Z, Kanapeckaitė S, Pileckienė J, Stalnionis G (2011) Russ J Electrochem 47:129
26. Survilienė A, Survila A (2002) Russ J Electrochem 38:1216
27. Būdienė J, Kalinauskas P, Survila A (2004) Chemija (Vilnius) 15:7
28. Pileckienė J, Grigucevičienė A, Survila A (2011) Chemija (Vilnius) (in press)
29. Survila A, Baliukienė V (2001) Chemija (Vilnius) 12:195
30. Macdonald JR (1987) Impedance spectroscopy. Wiley, New York
31. Lasia A (1999) Electrochemical impedance spectroscopy and its applications. In: Konway BE, Bocris J, White RE (eds) Modern aspects of electrochemistry, vol 32. Kluwer Academic/Plenum, New York, p 143